Aspect-ratio and lateral-resolution enhancement in force microscopy by attaching nanoclusters generated by an ion cluster source at the end of a silicon tip

L. Martínez,[1] M. Tello,[2] M. Díaz,[1] E. Román,[1] R. Garcia,[2] and Y. Huttel[1]
[1]*Instituto de Ciencia de Materiales de Madrid, Consejo Superior de Investigaciones Científicas (CSIC) C/ Sor Juana Inés de la Cruz, 3 28049 Madrid, Spain*
[2]*Instituto de Microelectrónica de Madrid (CSIC), Isaac Newton 8 (PTM), 28760 Tres Cantos, Madrid, Spain*

(Received 12 November 2010; accepted 30 January 2011; published online 28 February 2011)

One of the factors that limit the spatial resolution in atomic force microscopy (AFM) is the physical size of the probe. This limitation is particularly severe when the imaged structures are comparable in size to the tip's apex. The resolution in the AFM is usually enhanced by using sharp tips with high aspect ratios. In the present paper we propose an approach to modify AFM tips that consists of depositing nanoclusters on standard silicon tips. We show that the use of those tips leads to atomic force microscopy images of higher aspect ratios and spatial resolution. The present approach has two major properties. It provides higher aspect-ratio images of nanoscale objects and, at the same time, enables to functionalize the AFM tips by depositing nanoparticles with well-controlled chemical composition. © *2011 American Institute of Physics*. [doi:10.1063/1.3556788]

I. INTRODUCTION

The spatial resolution of nanoscale structures in the atomic force microscopy (AFM) is highly dependent on the geometry of the tips. The convolution of the tip and structure geometries[1–8] determine the final image. As a consequence the measured lateral size is usually larger than the true size. Furthermore, this effect could lead to a loss in spatial resolution[6,7] (see Fig. 1). The lateral resolution l between two sharp features imaged by a parabolic tip with end radius R can be defined[6,7] as

$$l = \sqrt{2R}\,(\sqrt{\delta h_r} + \sqrt{\delta h_r + \Delta h}),$$

where Δh is the height difference existing between the adjacent features and δh_r is the vertical resolution. Tips with higher aspect ratios (ratio between the height and the width of the tips apex) enable improving spatial resolution and contrast. Hence the geometry of the tips for scanning probe microscopies is a key point and the fabrication of high-aspect-ratio tips is an important issue for these techniques and, in particular, for AFM. Usually the AFM tips are pyramids with square bases and a mean radius of around few nanometers. The tips can be excited to their resonant frequency in the so-called dynamic modes, where contact between tip and sample is reduced, and therefore, tip and sample life can be extended.[9–14] Silicon tips with higher aspect ratios are also available, although their individual processing by ion milling, for example, drastically increases their cost and their fragility as compared to etched silicon tips. Several alternative procedures have been developed to either reduce the tips radius and/or to get better aspect ratios.[12,15–18] The formidable aspect ratio as well as the small diameter of single wall carbon nanotubes (SWCNTs) makes them seemingly ideal candidates for AFM imaging.[16,18,19]

Advanced AFM users very often modify the tips in order to functionalize them for specific applications and measurements.[20,21] This is also the case in magnetic force microscopy,[22,23] where the silicon tips are coated with a magnetic material with defined magnetic properties such as coercive field. These tip modifications are not oriented to increase the aspect ratio of the tips but rather to provide them with other physical properties of interest such as magnetic or piezoelectric interactions through the modification of the chemical composition.[24] Furthermore, the modification processes to reach specific physical properties can reduce the aspect ratio.[25,26]

Here we present a new method for both the functionalization and reduction of the final radius of tips that can be used in scanning probe microscopies. We will focus our study on the increase of the aspect ratio of the imaged nanostructures through the modification of silicon tips by deposition of nanoclusters under ultrahigh vacuum (UHV) conditions using an ion cluster source (ICS).[27] A significant increase of the resolution can be obtained by depositing nanoparticles of a few nanometers diameter that are located at the end of the tips and act as the ultimate atomic force probe. The measured objects interact primarily with the part of the tip that is closer to the surface, i.e., in the case of the modified tips, with the deposited nanoparticle that is emerging from the tip. Reducing the size of the probe leads to an enhancement of the resolution that together with the ability to tune the physical and chemical properties of the tips by depositing nanoparticles with controlled and variable chemical composition[28] are the main properties of the present tips modification method.

II. EXPERIMENTAL DETAILS

All the AFM tips were purchased from Nanosensors[29] (Pointprobe-Plus noncontact/tapping mode high resonance frequency, resonant frequency: 270–310 kHz, and nominal force constant: 10–130 N/m), and the AFM measurements were performed in the amplitude modulation AFM mode using a Nanoscope IIIa (Veeco Instruments).[30] Some tips were

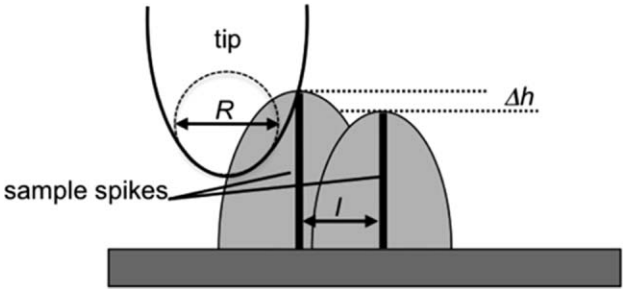

FIG. 1. Scheme of the AFM imaging process performed by a parabolic tip of radius of curvature *R* over two sharp spikes. The minimum lateral separation between the spikes depends on the height difference that exists between the adjacent features.

used directly to record reference images on selected areas of reference patterns. It should be noted that the standard silicon tips have aspect ratios that can change from tip to tip even in the same production series. In our case we have tested a series of standard silicon tips and used only the standard silicon tips with the best performances. AFM images were recorded on the same areas with other AFM tips that were previously modified by depositing a multilayer of nanoclusters using an ion cluster source[31] attached to an UHV chamber. In this UHV chamber the base pressure was in the middle 10^{-10} mbar and in the middle 10^{-5} mbar during the deposition of the clusters. The tips were transferred into the UHV chamber through a fast entry chamber. Series of depositions on the tips were performed in order to deposit nanoclusters of nominal diameter of 2–3 nm and 6–7 nm (from now on called T-3nm and T-7nm). The different parameters of the ICS (mainly He and Ar fluxes, applied magnetron power, and aggregation length) were adjusted to obtain the desired diameters, and the size of the clusters was checked systematically. The target material used in the magnetron was $Co_{95}Au_5$. Several tests performed with different coverages of nanoparticles have shown that the minimum nominal cluster coverage is around five monolayers of clusters on the AFM tips. Lower coverages lead to nonreproducible tips, i.e., tips that not always allow an increased lateral resolution when performing imaging. This is due to the fact that the spatial distribution of the nanoparticles is random, and therefore, a minimum of five nanoparticle-layer (nominal coverage) is needed in order to ensure that the very end of the apex is covered by at least one particle in most of the cases. The formation of double tip was observed in a very limited number of modified tips. As with standard tips, a double tip could be "repaired" by briefly pushing the tip into the surface using a small and controlled force.

The chosen patterns for the measurements were zero-dimensional, one-dimensional, and two-dimensional systems that have low dimensional structures that are frequently measured in AFM. In our case we have measured the following systems: (1) submonolayer of 10 nm diameter $Co_{95}Au_5$ clusters deposited on a flat silicon wafer surface, (2) single wall carbon nanotubes deposited on a flat silicon wafer,[32] and (3) ordered macroporous Ce–Zr mixed oxides.[33,34] The images were taken at a scanning rate of 1 Hz, with a pixel resolution of 512 × 512 in the *X* and *Y* axes and 1 μm × 1 μm scanning size. In some cases, a zoom of the desired area has been taken from the original picture in order to get a clearer view of the region of interest.

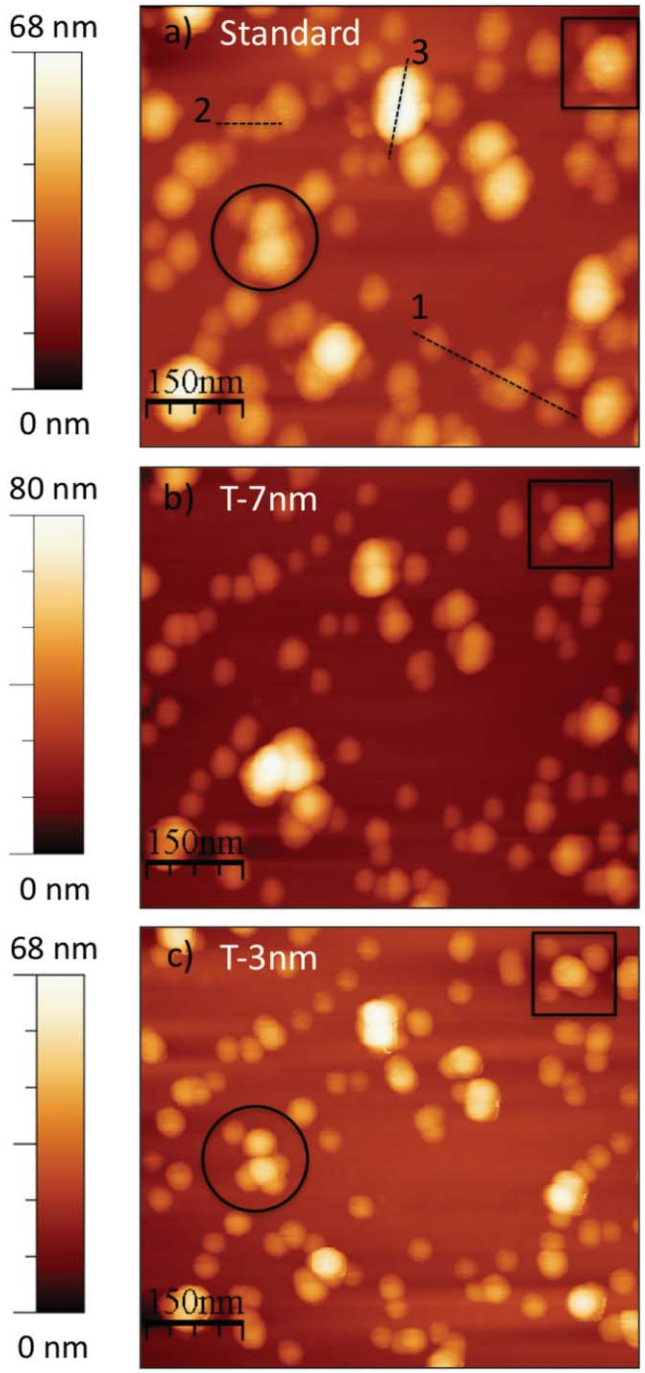

FIG. 2. (Color online) AFM images of $Co_{95}Au_5$ nanoclusters generated by an ion cluster source and deposited on a silicon wafer. (a) AFM image recorded by using a standard silicon AFM tip; (b) AFM image recorded by using a standard silicon AFM tip covered with 6–7 nm nanoparticles; and (c) AFM image recorded by using a standard silicon AFM tip covered with 2–3 nm nanoparticles. The size of the images is 750 × 640 nm^2.

III. RESULTS AND DISCUSSION

We will first focus on the evolution of the AFM images recorded on the 10 nm diameter clusters (nominal value) deposited on a flat silicon surface. Note that the nanoclusters

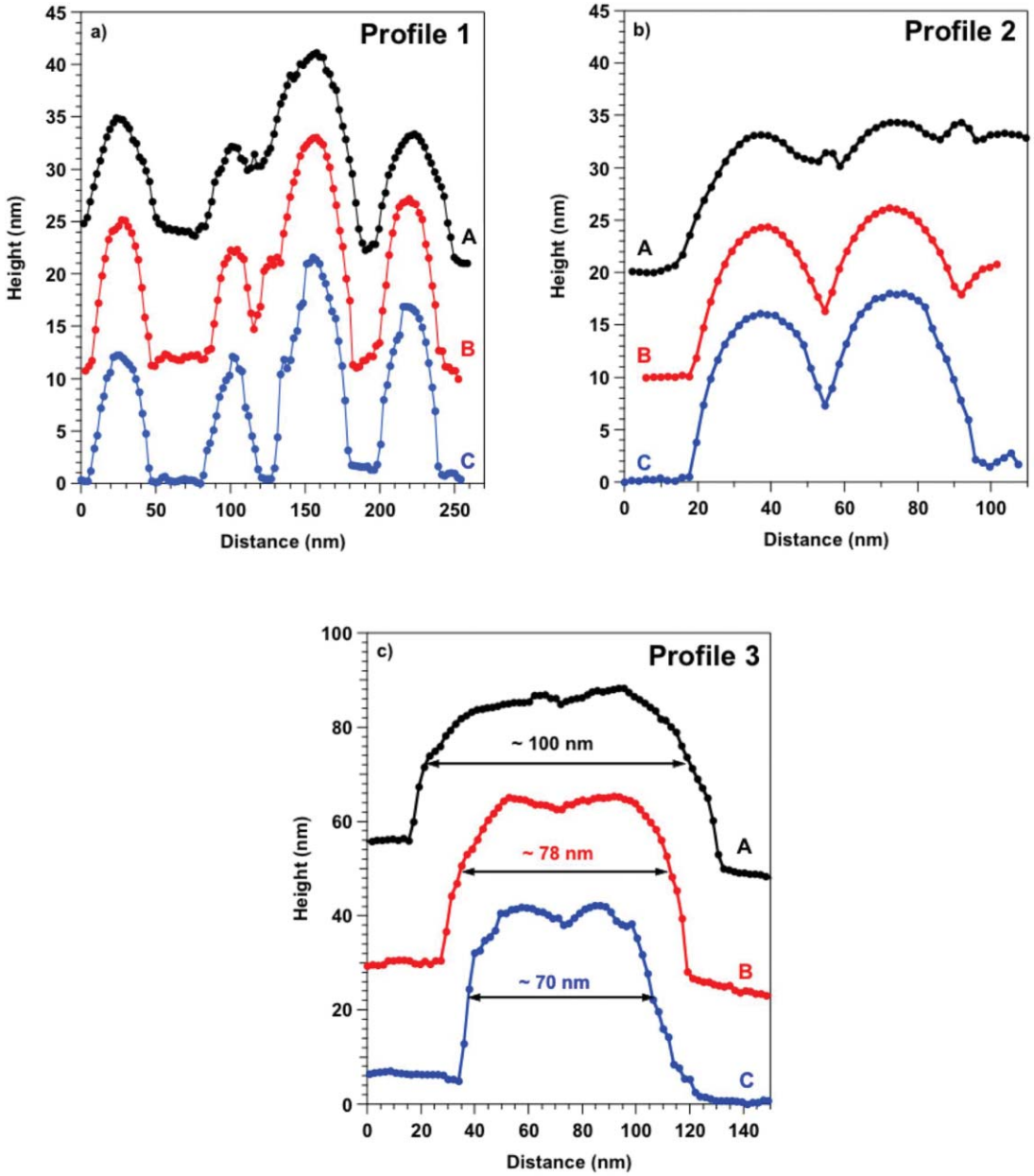

FIG. 3. (Color online) Profiles extracted from AFM images acquired on the nanoparticles deposited on a silicon surface for different tips. [(a)–(c)] Profiles extracted from lines indicated as 1, 2, and 3, respectively, in Fig. 2(a). The profiles extracted from the reference pattern recorded with the nonmodified tip are labeled A, while the profiles extracted from the images recorded with the T-7 nm and T-3 nm tips are labeled B and C, respectively. Different offsets have been added to profiles A and B in order to facilitate the comparison.

deposited on the silicon surface are the same type of clusters that have been deposited on the tips, although the nominal size is different. The images are displayed in Fig. 2 and correspond to (a) AFM image recorded with a standard nonmodified (commercial) silicon tip, (b) AFM image recorded with the T-7nm nanocluster tip (silicon tip covered with 6–7 nm nanoparticles), and (c) AFM image recorded with the T-3nm nanocluster tip (silicon tip covered with 2–3 nm diameter nanoparticles). The imaged areas are the same in all the three images displayed in Fig. 2. A reduction in the feature size and an increase of the in-plane contrast and resolution are appreciated in the AFM images from top to bottom. Several features of the image recorded with the nonmodified tip exhibit more complex structures when measured with the modified tips. This is the case of the nanoparticle that is indicated in the square frame. This nanoparticle presents a structure that is hardly distinguishable in Fig. 2(a); however, four minor features are clearly resolved in Fig. 2(b) and well defined in Fig. 2(c), where five nanoparticles are observable. Also better resolved in Fig. 2(c) is the nanostructure inside the marked circle. In Fig. 2(a), such nanostructure appears as a broad aggregate, while the use of a sharper tip reveals the presence of six nanoparticles [Fig. 2(c)]. Note that this structure appears displaced in Fig. 2(b). The displacement of the nanostructures can also be observed in other regions of the images. It could be attributed to a tip effect, although the

measurements have been performed by applying a low force. We have to bear in mind that the imaged nanoparticles are similar to the ones attached to the tip, so it is likely that some of them can be dragged away while scanning.

It therefore appears that the nanostructures become better resolved by decreasing the diameter of the nanoclusters deposited on the corresponding silicon tips. Consequently, the deposition of nanoclusters on the standard silicon tips induces an increase of the resolution in the AFM imaging. In order to quantify such effect, selected profiles represented by dashed lines in Fig. 2(a) have been extracted and are presented in Fig. 3 [profiles A, B, and C were extracted from Figs. 2(a), 2(b) and 2(c), respectively].

In Fig. 3(a) it can be observed that the resolution increases from profile A to profile B, where the structures between 80 and 140 nm are resolved when the image is recorded with the T-7nm, while those structures are not resolved with the nonmodified tip. The effect of the modification of the tip on the resolution is even higher when depositing nanoparticles of 2–3 nm diameter. This can be appreciated when comparing profiles B and C in Fig. 3(a), where the structures between 80 and 140 nm are resolved in profile C with a well defined separation at 125 nm. The aspect ratio of the imaged nanostructures is also improved with the nanoscluster tips. This effect can be appreciated with the profiles of Fig. 3(a), where in profile C the tip reaches the flat silicon wafer substrate, as can be observed at distances at around 70, 125, 190, and 250 nm, while this is not the case for profile A. As expected, profile B is an intermediate stage between profiles A and C. This shows that the resolution is directly correlated with the size of the nanoparticles deposited on the silicon tips apex. The clear distinction between features close to each other as a function of the size of the nanoparticles deposited on the tips can also be observed in Fig. 3(b), where we display the profiles of point 2 [cf. Fig. 2(a)]. As can be observed, while profile A shows a broad structure, profiles B and C allow a clear distinction between the two nanoparticles in the profile. In Fig. 3(c) we present the profiles extracted from point 3 of Fig. 2(a). The full width at half maximum (FWHM) has been estimated for each profile assuming a Gaussian fit. Compared to the structure of profile 1 [cf. Fig. 3(a)], the size of the feature of profile 3 is relatively large. Nevertheless, the effect of the different tips is still clearly observable. The use of a tip covered with 6–7 nm nanoparticles induces a reduction of 22% of the apparent diameter of the measured feature, and the use of a tip covered by 2–3 nm nanoparticles induces an additional reduction of the apparent diameter by 8%. This increase of the resolution as a function of size of nanoparticles deposited on the tips clearly shows that the effect on the resolution is associated with the deposited nanoparticles and their diameter.

So far we have studied the performance of the nanoclusters tips on the resolution of the images acquired on zero-dimensional systems (nanoparticles deposited on a flat silicon wafer). We will now focus on the evolution of the resolution when measuring well defined one-dimensional structures such as SWCNTs deposited on a flat silicon wafer. In this case, the diameter of the structure is well defined[35] and the SWCNTs are anchored to the silicon surface by

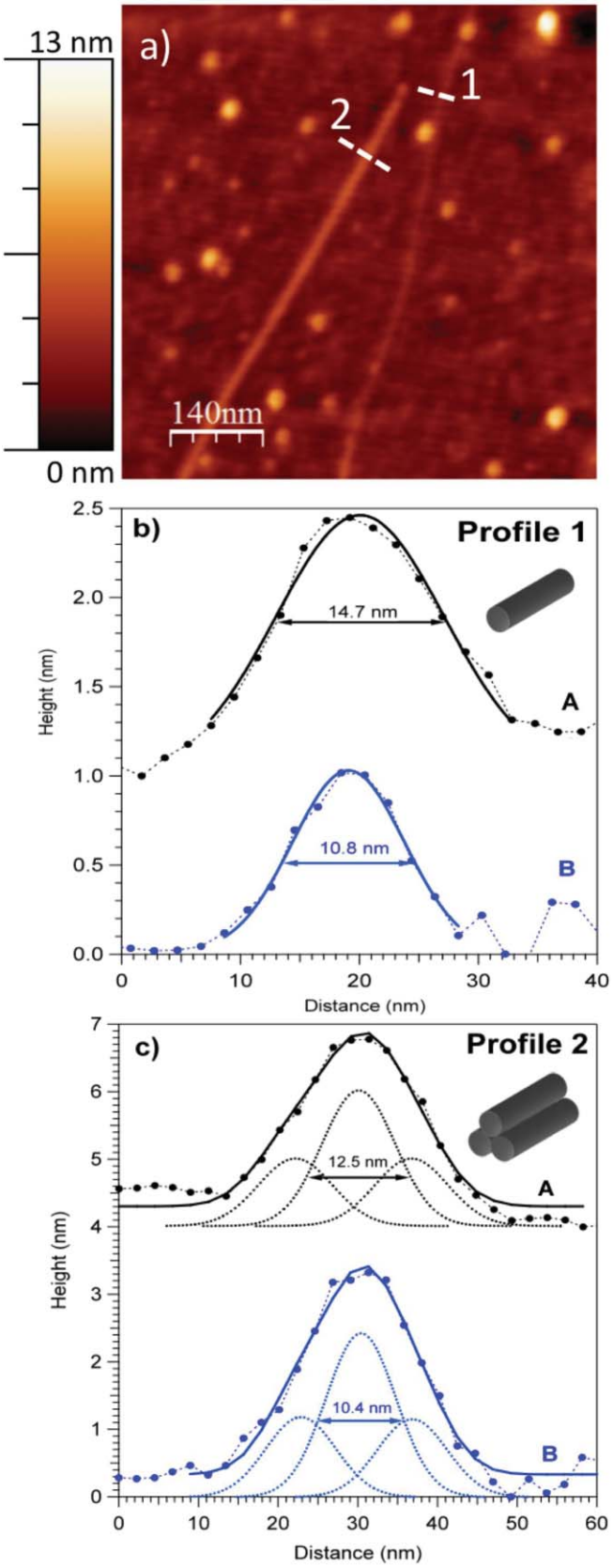

FIG. 4. (Color online) (a) AFM image of single wall carbon nanotubes deposited on a flat silicon wafer. (b) Profiles extracted at point 1 of (a). A corresponds to profile measured with the nonmodified tip (an offset of 1 nm has been added for clarity) and B to the one measured with T-3nm. (c) Same as (b) but with profile extracted at point 2 from (a). For clarity, an offset of 4 nm has been added in the case of profile A. The size of the images is 700 × 700 nm^2.

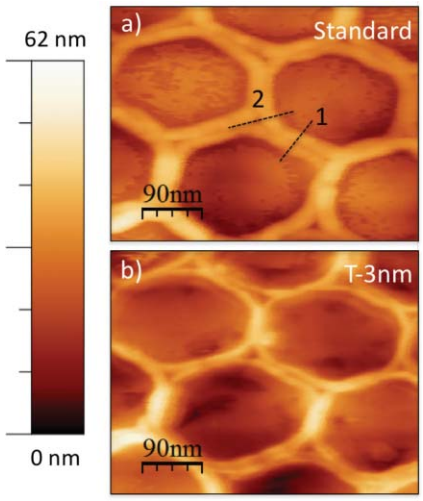

FIG. 5. (Color online) AFM images of inverse-opal. (a) AFM image recorded using a standard silicon AFM tip; (b) AFM image recorded using a commercial tip covered by 2–3 nm nanoparticles. The size of the images is $460 \times 350\ \text{nm}^2$.

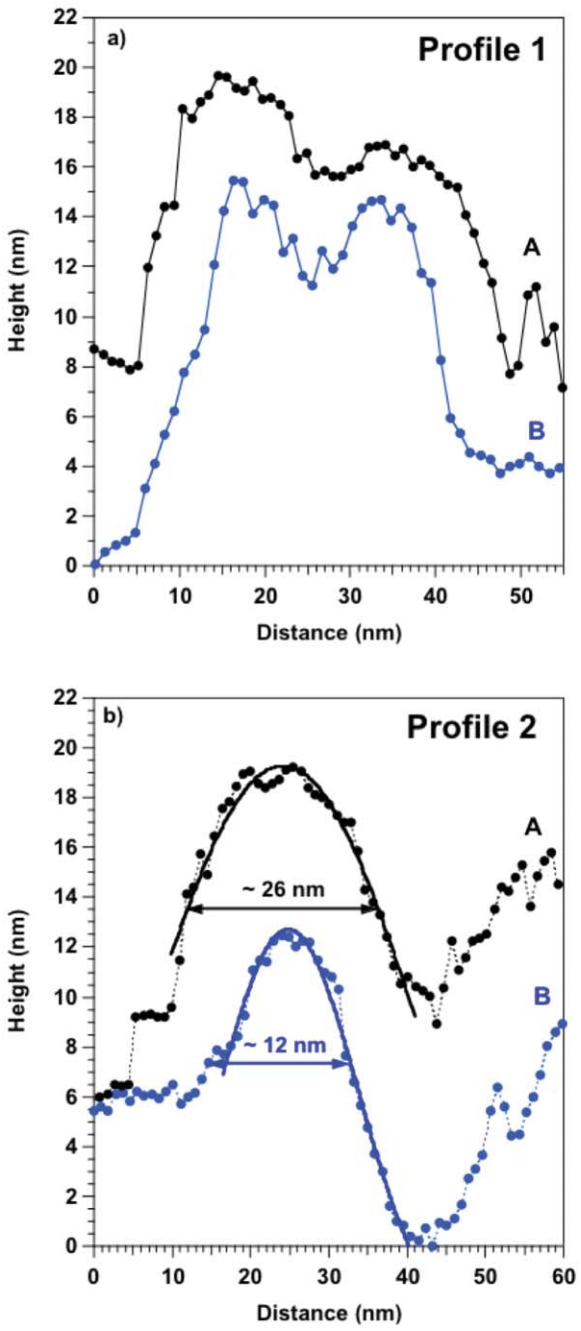

FIG. 6. (Color online) Profiles extracted from AFM images displayed in Fig. 5. (a) Profiles extracted from line indicated as 1 in Fig. 5(a); (b) Profiles extracted from line indicated as 2 in Fig. 5(a).

electrostatic forces through the use of an appropriate layer of molecules.[36] Such electrostatic anchoring is likely to prevent their displacement during the measurement in the amplitude modulation AFM mode.

The AFM images were recorded with the nonmodified and nanoparticle coated tips. In the case of SWCNT deposited on a flat silicon surface, no drastic enhancement of the resolution in the AFM images could be directly observed, probably due to the very low dimensions of the measured objects. We therefore present only the image measured with the T-3nm that is displayed in Fig. 4(a). Measurements have been performed on many different areas of the sample, and the analysis of the effect of the modification of the tips has been performed on many SWCNTs. The results presented in Fig. 4 are representative of all these measurements and analysis. In Fig. 4(a) we have highlighted two cross-section points (labeled 1 and 2) where profiles have been extracted and represented in Figs. 4(b) and 4(c), respectively. When performing such profiles, the difficulties arise from the fact that the measured structures are very small and the choice of the cross-section point is mandatory in order to obtain profiles with relatively flat background where the relevant information on the FWHM can be extracted in a reliable way. This has been performed in profiles of Figs. 4(b) and 4(c). These profiles are representative of other profiles that have been measured at other cross-section points and that gave similar results. Profiles of Fig. 4(b) have been performed on the thinnest SWCNT of Fig. 4(a). The height of the profiles, which is 1.0–1.2 nm, suggests that the measured structure corresponds to an isolated SWCNT. From the Gaussian fits, FWHM of 14.7 and 10.8 nm is extracted from the AFM images recorded, respectively, with the nonmodified tip and the T-3nm. This result confirms the enhanced resolution obtained with the nanoparticle coated tips. Profiles of Fig. 4(c) are representative of those extracted from the bigger structure present in Fig. 4(a). From the height of the profiles (2.7–3.1 nm) it is suggested that such structure corresponds to three SWCNTs piled up, as depicted in Fig. 4(c). Also the shoulders in the profiles of Fig. 4(c) suggest the presence of such pile up of three SWCNTs. Assuming such a structure, the profiles have been fitted with three Gaussian components. The width of the Gaussian components of each profile has been fixed to the same value. This resulted to a FWHM of each component to 12.5 and 10.4 nm for profiles extracted from images recorded with the nonmodified tip and 3-nm AFM tip, respectively. In Fig. 4(b) the reduction of the FWHM of the measured SWCNT (comparing the measurements performed with the nonmodified tip with those performed with the T-3nm) is approximately 26%, which is very similar to the reduction of the FWHM observed in the

case of zero-dimensional structures. The observed reduction of the FWHM in other cross-section points of the SWCNT was ranging from 14% to 37 % in the best cases. When comparing the FWHM of the SWCNT measured with the non-modified tip and the T-7nm, the reduction was found to be 19% in the best cases.

Finally, we have also recorded AFM images on a two-dimensional system made of ordered macroporous Ce–Zr mixed oxides[33,34] that display an hexagonal array. The corresponding images are displayed in Fig. 5. Here, we display only the image recorded with the standard silicon tip (top image) and the T-3nm (bottom image). The imaged areas are the same in all the two images displayed in Fig. 5. A qualitative enhancement of the resolution of the recorded image is again appreciable by the use of the modified tip. The walls that separate the hexagons are better defined in the bottom image. This effect is quantified by means of profiles that are displayed in Fig. 6 and correspond to the lines depicted in Fig. 5(a). Profile 1 is represented in Fig. 6(a). In Fig. 6 an offset has been applied in order to facilitate the comparison. It clearly appears that curve B is narrower than curve A as a result of a better resolution. The enhancement of the resolution is better appreciated in profile 2, where we have fitted the curves using a Gaussian function (cf. Fig. 6). It appears that the FWHM is drastically reduced by more than 50% with the use of a modified T-3nm. These results confirm that the proposed procedure to enhance the resolution of the AFM measurements is also applicable to two-dimensional systems. It should be mentioned that in this paper we have chosen to deposit nanoparticles as small as 2–3 nm diameter, but the parameters of the ion cluster source can be adjusted to produce smaller nanoparticles that could be deposited on tips to push forward the resolution of the measurements. It is also interesting to note that the use of tips covered by well-defined nanoclusters allows a better reproducibility of the measurements compared to the standard silicon tips whose shape might vary from tip to tip. We also note that the lifetime of the tips is increased after deposition of the nanoparticles.

IV. CONCLUSIONS

We have studied the performance of tips modified by the deposition of nanoparticles on standard silicon tips. By imaging zero-, one-, and two-dimensional structures we have shown that the use of tips coated with either nanoparticles of 6–7 nm or 2–3 nm in nominal diameter produces a significant enhancement of the features' aspect ratio. Additionally, we have demonstrated that the effect on the lateral resolution is directly correlated with the size of the nanoparticles that are deposited on the tips. Smaller nanoparticles produce images with higher aspect ratios. The presented tips modification method represents an alternative for the generation of high-aspect-ratio tips for high resolution measurements. It should be mentioned that the modification of tips by depositing nanoclusters is a "one step process" that does not need any additional chemical of physical process. Furthermore, the ability to tune the chemical composition of the deposited nanoparticles implies that the technique can be extended for specific measurements in other force microscopy techniques such as magnetic force microscopy.

ACKNOWLEDGMENTS

The authors acknowledge the Spanish Ministerio de Ciencia e Innovación and Comisión Interministerial para la Ciencia Y la Tecnología—CICYT under Contract Nos. MAT2008-06765-C02-02, MAT2009-08650, and CSD2007 00041 (Nanoselect) and through the FPI and "Juan de La Cierva" programs for financial support. Professor Julio Gómez Herrero (Laboratorio de Nuevas Microscopías, Dep. Física de la Materia Condensada, Universidad Autónoma de Madrid, Spain) and Dr. Dino Tonti (ICMM) are acknowledged for the preparation of the single wall carbon nanotubes and ordered macroporous Ce–Zr mixed oxides samples, respectively. The Consejo Superior de Investigaciones Científicas is also acknowledged.

Free nanoparticle coating of AFM tips can be obtained upon request to huttel@icmm.csic.es.

[1] D. J. Keller and F. S. Franke, Surf. Sci. **294**, 409 (1993).
[2] X. Qian and J. S. Villarrubia, Ultramicroscopy **108**, 29 (2007).
[3] P. E. Mazeran, L. Odoni, and J. L. Loubet, Surf. Sci. **585**, 25 (2005).
[4] A. Yacoot and L. Koenders, J. Phys. D: Appl. Phys **41**, 103001 (2008).
[5] Q. Zia and R. Androsch, Meas. Sci. Technol. **20**, 097003 (2009).
[6] R. Garcia, *Amplitude Modulation Atomic Force Microscopy* (Wiley-VCH, Weinheim, 2010).
[7] C. Bustamante and D. Keller, Phys. Today **48**(12), 32 (1995).
[8] Y. Gan, Surf. Sci. Rep. **64**, 99 (2009).
[9] A. San Paulo and R. Garcia, Phys. Rev. B **64**, 193411 (2001).
[10] S. Akita, Y. Nakayama, S. Mizooka, Y. Takano, T. Okawa, and T. Nosaka, Appl. Phys. Lett. **79**, 1691 (2001).
[11] P. A. Williams, S. J. Papadakis, M. R. Falvo, S. Washburn, and R. Superfine, Appl. Phys. Lett. **80**, 2574 (2002).
[12] E. S. Snow, P. M. Campbell, and J. P. Novak, Appl. Phys. Lett. **80**, 2002 (2002).
[13] S. Akita and Y. Nakayama, Jpn. J. Appl. Phys. **41**, 4887 (2002).
[14] N. De Jonge, Y. Lamy, and M. Kaiser, Nano Lett. **3**, 1621 (2003).
[15] D. J. Keller and C. C. Chou, Surf. Sci. **268**, 333 (1992).
[16] C. L. Cheung, J. H. Hafner, and C. M. Lieber, Proc. Natl. Acad. Sci. U.S.A. **97**, 3809 (2000).
[17] D. Klinov and S. Magonov, Appl. Phys. Lett. **84**, 2697 (2004).
[18] J. Martinez, T. D. Yuzvinsky, A. M. Fennimore, A. Zettl, R. Garcia, and C. Bustamante, Nanotechnology **16**, 2493 (2005).
[19] S. S. Wong, A. T. Woolley, E. Joselevich, and C. M. Lieber, Chem. Phys. Lett. **306**, 219 (1999).
[20] P. Hinterdorfer and Y. F. Dufrene, Nat. Methods **3**, 347 (2006).
[21] A. R. Bizzarri and S. Cannistraro, Chem. Soc. Rev. **39**, 734 (2010).
[22] T. Wang, Y. Wang, Y. Fu, T. Hasegawa, F. S. Li, H. Saito, and S. Ishio, Nanotechnology **20**, 105707 (2009).
[23] F. Wolny, T. Mühl, U. Weissker, K. Lipert, J. Schumann, A. Leonhardt, and B. Büchner, Nanotechnology **21**, 435501 (2010).
[24] A. G. Macedo, D. Ananias, P. S André, R. A Sa Ferreira, A. L Kholkin, L. D. Carlos, and J. Rocha, Nanotechnology **19**, 295702 (2008).
[25] A. Geissler, M.-F. Vallat, L. Vidal, J.-C. Voegel, J. Hemmerle, P. Schaaf, and V. Roucoules, Langmuir **24**, 4874 (2008).
[26] Q. K. Ong and I. Sokolov, J. Colloid Interface Sci. **310**, 385 (2007).
[27] E. L. Román García, L. Martínez Orellana, M. Díaz Lagos, and Y. Huttel, Spanish Patent No. P201030712 (filed 13 May 2010).
[28] E. L. Román García, L. Martínez Orellana, M. Díaz Lagos, Y. Huttel, Spanish Patent Cooperation Treaty No. PCT/ES2011/070032 (filed 19 January 2010).
[29] See http://www.nanosensors.com for the description of the different tips commercialized by the company.

[30]See http://www.veeco.com for the description of the atomic force microscopes.
[31]See http://www.oaresearch.co.uk for the description of the commercial Ion Cluster Source.
[32]V. López, L. Welte, M. A. Fernández, M. Moreno-Moreno, J. Gómez-Herrero, P. J. de Pablo, and F. Zamora, J. Nanosci. Nanotechnol. **9**, 2830 (2009).
[33]D. Tonti, M. J. Torralvo, E. Enciso, L. Martínez, E. Román, and J. Sanz, ECS Trans. **25**, 1573 (2009).
[34]D. Tonti, L. Martínez, M. J. Torralvo, E. Enciso, E. Román, and J. Sanz, J. Electrochem. Soc. **157**, B1499 (2010).
[35]D. G. Vercosa, E. B. Barros, A. G.Souza Filho, J. Mendes Filho, Ge. G. Samsonidze, R. Saito, and M. S. Dresselhaus, Phys. Rev. B **81**, 165430 (2010).
[36]Prior to the deposition of the nanotubes, the silicon wafers have been covered by a layer of aminopropiltrietoxisilane (APTS). A complete description of the preparation procedure can be found in the Ph.D. dissertation of C. Gómez-Navarro, "Medidas de transporte electrónico en cables moleculares: nanotubos de carbono y ADN," Ph.D. dissertation, Departamento de Física de la Materia Condensada, Universidad Autónoma de Madrid, Spain, October 2005. The dissertation can be obtained at ⟨http://dl.dropbox.com/u/7083540/TesisCristina1.pdf⟩.